Parton Radiation and Fragmentation from LHC to FCC-ee

Workshop Proceedings, CERN, Geneva, Nov. 22nd–23th, 2016

Editors

David d'Enterria (CERN), Peter Z. Skands (Monash)

Authors

D. Anderle (U. Manchester), F. Anulli (INFN Roma), J. Aparisi (IFIC València),
G. Bell (U. Siegen), V. Bertone (NIKHEF, VU Amsterdam), C. Bierlich (Lund Univ.),
S. Carrazza (CERN), G. Corcella (INFN-LNF Frascati), D. d'Enterria (CERN),
M. Dasgupta (U. Manchester), I. García (IFIC València), T. Gehrmann (U. Zürich),
O. Gituliar (U. Hamburg), K. Hamacher (B.U. Wuppertal), A.H. Hoang (U. Wien),
N.P. Hartland (NIKHEF, VU Amsterdam), A. Hornig (LANL Los Alamos),
S. Jadach (IFJ-PAN Krakow), T. Kaufmann (U. Tübingen), S. Kluth (T.U. München),
D.W. Kolodrubetz (MIT), A. Kusina (LPSC Grenoble), C. Lee (LANL Los Alamos),
G. Luisoni (CERN), V. Mateu (U. Salamanca), H. Matevosyan (U. Adelaide),
W. Metzger (Radboud U.), S.O. Moch (U. Hamburg), P.F. Monni (CERN),
B. Nachman (LBNL Berkeley), E.R. Nocera (U. Oxford), M. Perelló (IFIC València),
W. Placzek (Jagiellonian U., Kraków), S. Plätzer (IPPP Durham, U. Manchester),
R. Perez-Ramos (Paris), G. Rauco (U. Zurich), P. Richardson (CERN, IPPP-Durham),
F. Ringer (LANL Los Alamos), J. Rojo (NIKHEF, VU Amsterdam), Ph. Roloff (CERN),
Y. Sakaki (KAIST Daejeon), N. Sato (JLab Newport News), R. Simoniello (CERN),
T. Sjöstrand (Lund U.), P.Z. Skands (Monash U.), M. Skrzypek (INP Kraków),
G. Soyez (IPhT CEA-Saclay), I.W. Stewart (MIT), M. Stratmann (U. Tübingen),
J. Talbert (DESY, U. Oxford), S. Todorova (CNRS), S. Tokar (Comenius U.),
M. Vos (IFIC València), and A. Vossen (Indiana U.)

Abstract

This document collects the proceedings of the *"Parton Radiation and Fragmentation from LHC to FCC-ee"* workshop (`http://indico.cern.ch/e/ee_jets16`) held at CERN in Nov. 2016. The writeup reviews the latest theoretical and experimental developments on parton radiation and parton-hadron fragmentation studies –including analyses of LEP, B-factories, and LHC data– with a focus on the future perspectives reacheable in e^+e^- measurements at the Future Circular Collider (FCC-ee), with multi-ab^{-1} integrated luminosities yielding 10^{12} and 10^8 jets from Z and W bosons decays as well as 10^5 gluon jets from Higgs boson decays. The main topics discussed are: (i) parton radiation and parton-to-hadron fragmentation functions (splitting functions at NNLO, small-z NNLL resummations, global FF fits including Monte Carlo (MC) and neural-network analyses of the latest Belle/BaBar high-precision data, parton shower MC generators), (ii) jet properties (quark-gluon discrimination, e^+e^- event shapes and multi-jet rates at NNLO+N^{n}LL, jet broadening and angularities, jet substructure at small-radius, jet charge determination, e^+e^- jet reconstruction algorithms), (iii) heavy-quark jets (dead cone effect, charm-bottom separation, gluon-to-b$\bar{\text{b}}$ splitting); and (iv) non-perturbative QCD phenomena (colour reconnection, baryon and strangeness production, Bose-Einstein and Fermi-Dirac final-state correlations, colour string dynamics: spin effects, helix hadronization).

Speakers

D.P. Anderle (U. Manchester), F. Anulli (INFN Roma), V. Bertone (NIKHEF Amsterdam), C. Bierlich (Lund Univ.), G. Corcella (INFN-LNF Frascati), D. d'Enterria (CERN), M. Dasgupta (U. Manchester), K. Hamacher (Bergische U. Wuppertal), S. Jadach (IFJ-PAN Krakow), S. Kluth (T.U. München), W. Metzger (Radboud U.), V. Mateu (U. Salamanca), H. Matevosyan (U. Adelaide), S.O. Moch (U. Hamburg), P.F. Monni (CERN), B. Nachman (LBNL Berkeley), S. Plätzer (IPPP Durham, U. Manchester), R.Perez-Ramos (Paris), G. Rauco (U. Zurich), P. Richardson (CERN, IPPP-Durham), Y. Sakaki (KAIST Daejeon), N. Sato (JLab Newport News), M. Selvaggi (CERN), T. Sjöstrand (Lund U.), P.Z. Skands (Monash U.), G. Soyez (IPhT CEA-Saclay), J. Talbert (DESY), S. Todorova (CNRS), S. Tokar (Comenius U.), M. Vos (IFIC València), A. Vossen (U. Indiana)

Additional Participants

N.Alipour Tehrani (CERN), S. Amoroso (CERN), A. Blondel (U. Genève), H. Brooks (IPPP/Durham U.), S. Carrazza (CERN), M. Dam (Niels Bohr Institute), N. Fischer (Monash U.), O. Fischer (U. Basel), J. Gao (Jiao Tong U., Shanghai), P. Gunnellini (DESY), I. Helenius (Tübingen U.), P. Janot (CERN), A. Jueid (Essaadi U.), D. Kar (U. Witwatersrand), M. Klute (MIT), E. Leogrande (CERN), T. A. Lesiak (INP-PAS, Krakow), H. Li (Monash U.), D. Liberati (CNR, Roma), A. Lifson (ETH Zurich), E. Locci (CEA-Saclay), L. Lönnblad (Lund U.), J.J. Lopez-Villarejo (Lausanne), G. Luisoni (CERN), S. B. Nielsen (U. Copenhagen, Niels Bohr Institute), V. Okorokov (MEPhI Moscow), F. Piccinini (INFN Pavia), W. Placzek (Jagiellonian U. Krakow) R. Rahmat (U.Iowa), P. Rebello-Teles (CBPF Rio de Janeiro), S. Richter (UC London), J. Rojo (NIKHEF, VU Amsterdam), M. Seidel (CERN), G. G. Voutsinas (CERN), B. Webber (Cambridge), L. Zawiejski (IFJ PAN Krakow)

1   Introduction

The workshop *"Parton Radiation and Fragmentation from LHC to FCC-ee"* was held at CERN, Nov. 22–23, 2016, as part of the FCC-ee *QCD and γ-γ physics* working group activities in the context of the preparation of the FCC-ee Conceptual Design Report in 2017. The meeting brought together experts from several different fields to explore the latest developments on our theoretical and experimental understanding of parton radiation and fragmentation, organized along four broad sessions:

1. **Parton-to-hadron fragmentation functions**, covering splitting functions at NNLO, small-z NNLL resummations, global FF fits including Monte-Carlo and neural-network analyses of the latest Belle/BaBar high-precision measurements;

2. **Parton radiation and jet properties**, including talks on parton showers, quark-gluon discrimination, precision e^+e^- event shapes and multi-jet rates, jet substructure and small-radius jets, jet charge determination; determination, and e^+e^- jet reconstruction algorithms;

3. **Heavy-quark jets**, with talks on the dead-cone effect, charm-bottom separation, and gluon-to-$b\bar{b}$ splitting;

4. **Non-perturbative QCD phenomena**, with talks on colour reconnections, baryon and strangeness production, Bose-Einstein and Fermi-Dirac and final-state hadron correlations, and colour string dynamics: spin effects, helix hadronization.

About 65 physicists took part in the workshop, and 30 talks were presented. Slides as well as background reference materials are available on the conference website

$$\text{http://indico.cern.ch/e/ee\_jets16}$$

These proceedings represent a collection of extended abstracts and references for the presentations, plus a summary of the most important results and future prospects in the field. Contents of these proceedings will be incorporated into the FCC-ee Conceptual Design Report under preparation.

CERN, January 2017

Peter Skands
David d'Enterria

2   Proceedings Contributions

————————————

Towards a Neural Network determination of Pion Fragmentation Functions

Valerio Bertone[1,2], Stefano Carrazza[3], Emanuele R. Nocera[4],
Nathan P. Hartland[1,2], and Juan Rojo[1,2]

[1] Department of Physics and Astronomy, VU University Amsterdam,
De Boelelaan 1081, NL-1081, HV Amsterdam, The Netherlands,
[2] Nikhef, Science Park 105, NL-1098 XG Amsterdam, The Netherlands,
[3] Theoretical Physics Department, CERN, Geneva Switzerland,
[4] Rudolf Peierls Centre for Theoretical Physics, 1 Keble Road
University of Oxford, OX1 3NP, Oxford, United Kingdom.

Abstract: We present a first preliminary determination of a set of collinear fragmentation functions of charged pions based on the NNPDF methodology. This determination is based on a wide set of single-inclusive annihilation data, including the most recent and precise measurements from B-factory experiments. Our analysis is performed at leading, next-to-leading and next-to-next-to-leading order in quantum chromodynamics. We discuss the result of our fits, highlighting the quality of their description of the data and their stability upon inclusion of higher-order corrections.

Introduction

In the framework of quantum chromodynamics (QCD), fragmentation functions (FFs) encode the information on how quarks and gluons are turned into hadrons [1]. They are an essential ingredient in the factorisation theorems which allow for a quantitative description of hard-scattering processes involving identified hadrons in the final state [2]. Because of their nonperturbative nature, FFs are typically determined from the data in a global QCD analyses combining results from a variety of processes. These include hadron production in electron-positron single-inclusive annihilation (SIA), in lepton-nucleon semi-inclusive deep-inelastic scattering (SIDIS), and in proton-proton (pp) collisions (see *e.g.* Ref. [3]).

In this contribution, we present some recent progress towards a first determination of FFs and their uncertainties based on the NNPDF methodology. Within this methodology, FFs are represented as a Monte Carlo sample, from which the central value and the uncertainty can be computed respectively as a mean and a standard deviation, and they are parametrised by means of neural networks with a very large number of parameters (for details see *e.g.* Ref. [4] and references therein). As compared to the approach used in all the determinations of FFs achieved so far, the NNPDF methodology aims at reducing potential biases related to the procedure used to extract FFs. The NNPDF framework has proven to be robust, and has been extensively used to extract unpolarised [4] and polarised [5] parton distribution functions (PDFs) of the proton.

It looks then sensible to employ the NNPDF methodology to determine also FFs. The aim of this contribution is to begin such a program. To start with, here we limit our analysis to the FFs of charged pions, $\pi^{\pm}$, based on SIA data only. A dedicated forthcoming publication [6] will discuss these results for the pion FFs in more detail, as well as present results for the FFs of other light hadrons, namely charged kaons, $K^{\pm}$, and protons/antiprotons, $p/\bar{p}$, which constitute the largest fraction in frequently measured yields of hadrons. The discussion is organised as follows. First, we describe the dataset considered. Then, we discuss the theoretical framework and the settings adopted in our analysis. Finally, we present our set of pion FFs.

Experimental dataset

This determination of FFs is based on a comprehensive set of cross section data from electron-positron annihilation into charged pions. We include measurements from the experiments performed at CERN (ALEPH [7], DELPHI [8] and OPAL [9]), DESY (TASSO [10,11,12]), KEK (BELLE [13] and TOPAZ [14]), and SLAC (BABAR [15], HRS [16], TPC [17] and SLD [18]). On top of the inclusive measurements, we also include flavour-tagged SIA data from DELPHI [8], TPC [19] and SLD [18]. Specifically, we consider cross section measurements for the sum of light quarks (u, d, s) and for individual charm and bottom quarks (c, b).

The dataset included in this analysis is summarised in Tab. 1, where we specify the name of the experiments, their corresponding publication reference, the energy of the centre-of-mass system (c.m.s.) $\sqrt{s}$, the relative normalisation uncertainty (r.n.u.), and the number of data points included in the fit. The kinematic coverage of the dataset is displayed in Fig. 1.

The bulk of the dataset comes from the CERN-LEP and the SLAC-SLC experiments at the scale of the Z-boson mass, $\sqrt{s} = M_Z$ (ALEPH, DELPHI, OPAL and SLD), and from the B-factory experiments at a significantly lower c.m.s energy, $\sqrt{s} \simeq 10.5$ GeV (BELLE and BABAR). All these experiments provide very precise data, with relative uncertainties at the few percent level, which account for about two thirds of the total dataset. The remaining data points settle at intermediate energy scales and are typically affected by larger uncertainties.

Figure 1: The kinematic coverage in the $(z, \sqrt{s})$ plane of the SIA data in Tab. 1. The data is from DESY (black), KEK (green), SLAC (blue) and CERN (red).

In this analysis, we retain only the data which falls in the range $[z_{\min}, z_{\max}]$, with $z_{\min} = 0.05$ for the experiments at $\sqrt{s} = M_Z$ and $z_{\min} = 0.1$ for all the other experiments, and $z_{\max} = 0.9$ for all the experiments. These cuts are meant to exclude kinematic regions where resummation effects, not taken into account in our fixed-order analysis, may become relevant. The number of data points before kinematic cuts is reported in parentheses in Tab. 1.

We gather all the information on statistical and systematic uncertainties, including their correlations, whenever available, and construct the covariance matrix for each experiment accordingly. Possible normalisation uncertainties, given as a percentage correction to the measured observable (see Tab. 1), are assumed to be fully correlated. Because of their multiplicative nature, which would lead to a systematically biased result [20], they are included through an iterative procedure (the so-called t_0 method [21]). As usual in the NNPDF framework, the covariance matrix is used to sample the probability distribution defined by the data, by generating a Monte Carlo pool of $N_{\rm rep} = 100$ pseudodata replicas according to a multi-Gaussian distribution. A different fit to each pseudodata replica is then performed as described in the next section.
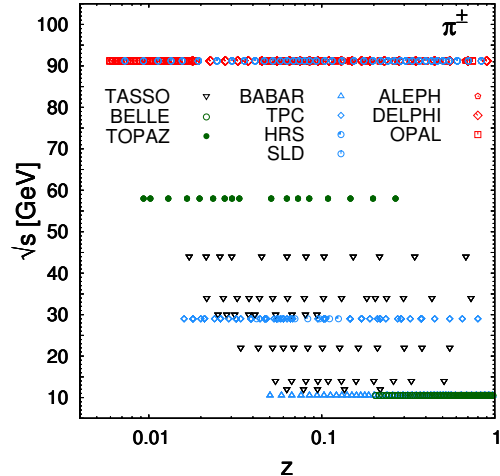
Exp.	Ref.	$\sqrt{s}$ [GeV]	r.n.u. [%]	N_{dat}	χ^2/N_{dat} (LO)	χ^2/N_{dat} (NLO)	χ^2/N_{dat} (NNLO)
BELLE	[13]	10.52	1.4	70 (78)	0.54	0.13	0.12
BABAR	[15]	10.54	0.098	37 (45)	1.04	1.28	1.37
TASSO12	[10]	12.00	20	2 (5)	0.71	0.88	0.84
TASSO14	[11]	14.00	8.5	7 (11)	1.54	1.60	1.68
TASSO22	[11]	22.00	6.3	7 (13)	1.28	1.65	1.62
TASSO34	[12]	34.00	6.0	8 (16)	1.09	1.08	0.99
TASSO44	[12]	44.00	6.0	5 (12)	1.96	2.00	1.85
TPC (incl.)	[17]	29.00	—	12 (25)	0.79	1.02	1.13
TPC (uds tag)	[19]	29.00	—	6 (15)	0.70	0.66	0.62
TPC (c tag)	[19]	29.00	—	6 (15)	0.74	0.75	0.76
TPC (b tag)	[19]	29.00	—	6 (15)	1.59	1.58	1.57
HRS	[16]	29.00	—	2 (7)	2.91	4.77	4.22
TOPAZ	[14]	58.00	—	4 (17)	1.03	0.94	0.81
ALEPH	[7]	91.20	3.0 - 5.0	22 (39)	0.78	0.64	0.68
DELPHI (incl.)	[8]	91.20	—	16 (23)	2.63	2.62	2.59
DELPHI (uds tag)	[8]	91.20	—	16 (23)	1.99	2.00	1.93
DELPHI (b tag)	[8]	91.20	—	16 (23)	1.13	1.00	1.14
OPAL	[9]	91.20	—	22 (51)	1.87	1.79	1.77
SLD (incl.)	[18]	91.20	1.0	29 (40)	0.71	0.71	0.70
SLD (uds tag)	[18]	91.20	1.0	29 (40)	0.81	0.78	0.80
SLD (c tag)	[18]	91.20	1.0	29 (40)	0.61	0.65	0.65
SLD (b tag)	[18]	91.20	1.0	29 (40)	0.45	0.60	0.46
Total				380 (602)	0.995	0.963	0.958

Table 1: The dataset included in this analysis of charged pion FFs. The experiment, the publication reference, the c.m.s. energy $\sqrt{s}$, the relative normalisation uncertainty (r.n.u.), the number of data points after (before) kinematic cuts, and the χ^2 per data point for the LO, NLO and NNLO analyses are displayed.

Theoretical framework and analysis settings

The leading observable in our analysis is the SIA cross section involving the production of a charged pion $\pi^\pm$ in the final state. This is usually defined in terms of the *fragmentation* (structure) function $F_2^{\pi^\pm}$ as:

$$\frac{d\sigma^\pm}{dz}(z, Q^2) = \frac{4\pi\alpha^2(Q^2)}{Q^2} F_2^{\pi^\pm}(z, Q^2)\,, \tag{1}$$

where $z = E^{\pi^\pm}/E_b = 2E^{\pi^\pm}/\sqrt{s}$ is the energy of the observed pion, $E^{\pi^\pm}$, scaled by the energy of the beam, E_b, and $Q^2 > 0$ is equal to the c.m.s. energy squared, s. At leading twist, the factorised expression of the inclusive $F_2^{\pi^\pm}$ is given as a convolution between FFs and coefficient functions, by:

$$F_2^{\pi^\pm} = \langle e^2 \rangle \left[D_\Sigma^{\pi^\pm} \otimes C_{2,q}^{\mathrm{S}} + n_f D_g^{\pi^\pm} \otimes C_{2,g}^{\mathrm{S}} + D_{\mathrm{NS}}^{\pi^\pm} \otimes C_{2,q}^{\mathrm{NS}} \right]\,, \tag{2}$$

where n_f is the number of active flavours, $\langle e^2 \rangle = n_f^{-1} \sum_q^{n_f} \hat{e}_q$ (with $\hat{e}_q$ the effective electroweak charges, see *e.g.* Ref. [22] for their definition), $D_\Sigma^{\pi^\pm} = \sum_q^{n_f} (D_q^\pi + D_{\bar{q}}^\pi)$ is the singlet FF, $D_{\mathrm{NS}}^{\pi^\pm} = \sum_q^{n_f} (\hat{e}_q^2/\langle e^2 \rangle - 1)(D_q + D_{\bar{q}})$ is a nonsinglet combination of FFs, $D_g^{\pi^\pm}$ is the gluon FF, and $C_{2,q}^{\mathrm{S}}$, $C_{2,q}^{\mathrm{NS}}$, and $C_{2,g}^{\mathrm{S}}$ are the corresponding coefficient functions (the explicit dependence on the scales has been omitted for brevity). From Eq. (2), it is apparent that inclusive SIA data can constrain only three independent distributions, namely $D_\Sigma^{\pi^\pm}$, $D_g^{\pi^\pm}$, and $D_{\mathrm{NS}}^{\pi^\pm}$. However, in the case of tagged data,

21

the sums on q inside Eq. (2) run only over tagged quarks. As a consequence, considering charm-and bottom-tagged data allows us to single out two more independent combinations of FFs.

In our analysis, we parametrise five independent FFs. On top of the singlet and the gluon FFs, $D_\Sigma^{\pi^\pm}$ and $D_g^{\pi^\pm}$, we choose the following nonsinglet combinations of FFs:

$$D_{T_3 + \frac{1}{3}T_8}^{\pi^\pm} = \frac{2}{3}(2D_{u^+}^{\pi^\pm} - D_{d^+}^{\pi^\pm} - D_{s^+}^{\pi^\pm}), \quad D_{T_{15}}^{\pi^\pm} = \sum_{q=u,d,s} D_{q^+}^{\pi^\pm} - 3D_{c^+}^{\pi^\pm}, \quad D_{T_{24}}^{\pi^\pm} = \sum_{q=u,d,s,c} D_{q^+}^{\pi^\pm} - 4D_{b^+}^{\pi^\pm}, \quad (3)$$

where $D_{q^+} = D_q + D_{\bar{q}}$. The contribution of heavy quarks fragmenting into light hadrons is not well described by perturbative DGLAP evolution, and thus heavy-quark FFs need to be extracted from data. Each FF in our basis is parametrised as $D_i^\pi(z, Q_0) = \mathrm{NN}_i(z) - \mathrm{NN}_i(1)$, $i = g, \Sigma, T_3 + \frac{1}{3}T_8, T_{15}, T_{24}$, where $\mathrm{NN}_i(z)$ are five independent neural networks (multi-layer feed-forward perceptrons) with 37 free parameters each. The subtraction of the term $\mathrm{NN}_i(1)$ ensures that $D_i^\pi(z = 1, Q_0) = 0$, as it should.

The FFs are evolved from the initial parametrisation scale Q_0 to the scale of the data by solving time-like DGLAP equations. We use the zero-mass variable-flavour-number (ZM-VFN) scheme, with up to $n_f = 5$ active flavours, in which heavy-quark mass effects in the partonic cross sections are not taken into account. We choose $Q_0 = 5$ GeV, above the charm and bottom masses, but below the lowest value of $\sqrt{s}$ for which SIA data is available. This way, we avoid to deal with cross sections near the heavy-quark thresholds, which would instead be better described in a matched general-mass VFN scheme [24], especially in the presence of intrinsic heavy-quark components.

Our analysis is performed at leading, next-to-leading and next-to-next-to-leading order (LO, NLO and NNLO) accuracy in perturbative QCD. The computation of the cross sections and the evolution of the FFs is performed with the APFEL program [25], and has been extensively benchmarked in Ref. [26]. We use the value $\alpha_s(M_Z) = 0.118$ as a reference for the running of strong coupling at the mass of the Z boson, $M_Z = 91.1876$ GeV, and the values $m_c = 1.51$ GeV and $m_b = 4.92$ GeV for the charm and bottom masses. We also take into account running effects of the fine-structure constant α to LO, taking $\alpha(M_Z) = 1/127$ as a reference value.

Our FFs are fitted to the data by means of a Covariance-Matrix-Adaptation Evolution-Strategy (CMA-ES) learning algorithm [23], which ensures an optimal exploration of the parameter space and an efficient χ^2 minimisation. In order to make sure that our fitting strategy provides a faithful representation of FFs and their uncertainties, we have validated it by means of *closure tests*. As discussed in detail in Ref. [4], closure tests are meant to quantify the robustness of the training methodology by fitting pseudodata generated using a given set of input FFs and checking whether the result of the fit is compatible with the input set. The successful outcome of our closure tests ensures that, in the region covered by the data included in the fit, procedural uncertainties (including those related to the parametrisation) are negligible, and that our extraction of FFs provides a faithful representation of the experimental uncertainties.

Results

We now present the results of our FF fits to charged pion data. In Tab. 1, we report the values of the χ^2 per data point for each experiment and for the whole dataset included in the fits corresponding to our LO, NLO, and NNLO analyses. We achieve a very good fit quality at all perturbative orders considered, with the global χ^2 being close to one in all cases. The inclusion of higher-order corrections improves the global description of the data noticeably when going from LO to NLO,
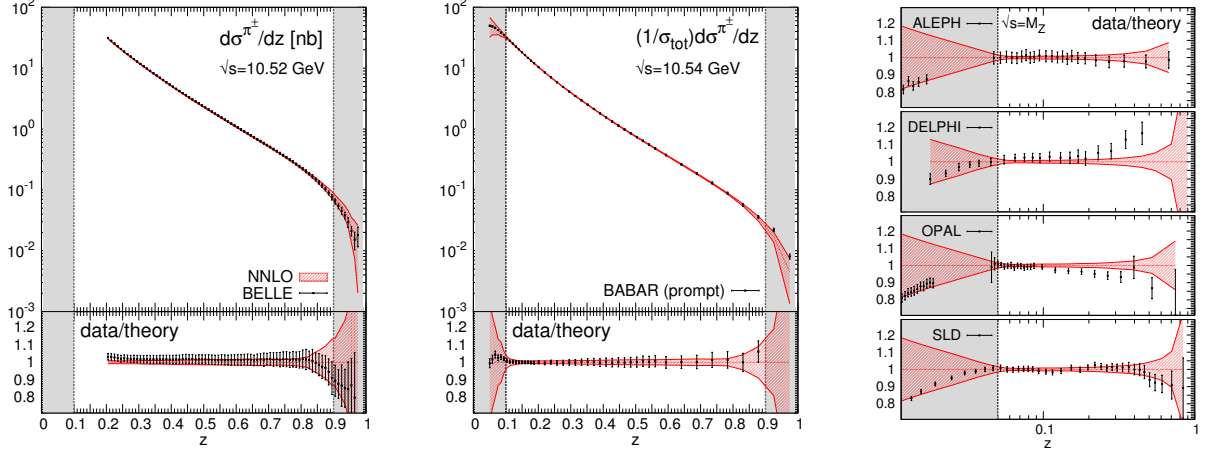
Figure 2: Data/theory comparison for BELLE (left), BABAR (center), and ALEPH, DELPHI, OPAL, and SLD (right) experiments. Predictions are obtained using our NNLO set of FFs. For BELLE and BABAR, we show both the original distributions (upper panel) and the data/theory ratio (lower panel); for the remaining experiments we show only the data/theory ratio. Shaded areas correspond to regions excluded by our cuts.

while only mildly when going from NLO to NNLO. In particular, the description of the BELLE measurements, which represent the most abundant and precise sample in our dataset, improves by a substantial amount. Simultaneously, the χ^2 to the BABAR data deteriorates as more higher-order corrections are included in the fit. This points to a possible tension between BELLE and BABAR measurements, as also suggested in a previous dedicated analysis [27].

In Fig. 2 we compare predictions obtained with our NNLO fit with the bulk of our dataset, namely the low-energy measurements ($\sqrt{s} \simeq 10.5$ GeV) from BELLE (left plot) and BABAR (central plot), and the measurements at $\sqrt{s} = M_Z$ from ALEPH, DELPHI, OPAL, and SLD (right plot). We display both the original distributions (upper panels) and the data/theory ratios (lower panels) for BELLE and BABAR, while only the ratio plots for the other experiments. In all plots, shaded areas indicate the kinematic regions excluded by our cuts.

In general, our predictions provide a fairly good description of all datasets, indicating that (N)NLO QCD is able to bridge low- and high-energy data without significant tension. As expected, the agreement between data and predictions in the region allowed by our cuts is particularly good with the only exception of DELPHI, whose large-z measurements tend to overshoot our predictions. This is reflected in the relatively poor χ^2 reported in Tab. 1. Remarkably, most of the measurements falling in the regions excluded by our kinematic cuts are compatible with our predictions that, however, are affected by larger uncertainties there. This suggests that, especially at small values of z, NNLO QCD is able to catch most of the beyond-fixed-order effects that our cuts are meant to keep under control (see also Ref. [28]). Consequently, our cuts might be unnecessarily restrictive at NNLO.

Finally, we turn to show the FFs resulting from our fits. From left to right, the plots in Fig. 3 show the singlet, $D_\Sigma^{\pi^\pm}$, the gluon, $D_g^{\pi^\pm}$, the total charm , $D_{c^+}^{\pi^\pm}$, and the total bottom, $D_{b^+}^{\pi^\pm}$, FFs at $Q = 10$ GeV. The upper panel of each plot shows our FFs at LO, NLO, and NNLO, while the lower panel displays the ratio to the corresponding LO distributions. The bands represent the one-σ uncertainty. These plots confirm our conclusions on the perturbative stability of our fits. In particular, we observe that in all cases the difference between LO and NLO is sizeable and the respective distributions are not compatible within uncertainty over most of the considered range in
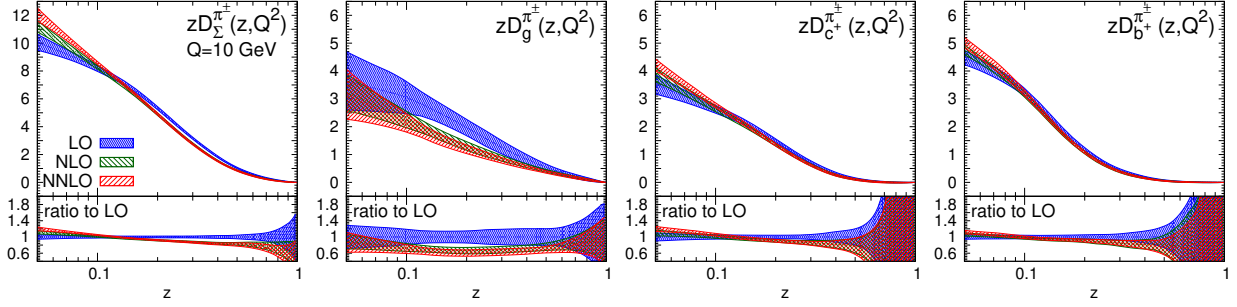
23

Figure 3: Comparison among our LO, NLO, and NNLO FFs at $Q = 10$ GeV. From left to right, the plots show the singlet $D_\Sigma^{\pi^\pm}$, the gluon $D_g^{\pi^\pm}$, the total charm $D_{c^+}^{\pi^\pm}$, and the total bottom $D_{b^+}^{\pi^\pm}$ FFs. The upper inset of each plot displays the FFs, while the lower inset displays their ratio to the corresponding LO FFs.

z. Conversely, the difference between NLO and NNLO is significantly smaller and the distributions are in much better agreement. We also note that the uncertainty band of the LO FFs is larger than that of the NLO and NNLO ones. A broadening of the uncertainties is indeed necessary to accommodate the absence of significant higher-order corrections. This effect, in conjunction with the deterioration of the χ^2, emphasises the inadequacy of the LO approximation.

Summary and outlook

We presented preliminary results of a determination of collinear FFs for charged pions based on the NNPDF methodology. The analysis was performed at LO, NLO, and NNLO in QCD and based SIA data only. We achieved a very good description of the data included in the fits and demonstrated perturbative convergence upon inclusion of higher-order corrections.

Our present results represent the first step towards a wider program. In the future, we plan to enlarge the fitted dataset by including hadron-production multiplicities in SIDIS and cross sections in pp collisions. This will allow for a separation between favoured and unfavoured FFs and for a clearer investigation of the flavour dependence of the FFs, aspects not directly accessible from SIA data. Further theoretical sophistications might include the assessment of heavy-quark and resummation effects, which might be significant [24,28].

References

[1] J. C. Collins and D. E. Soper, Nucl. Phys. B **193** (1981) 381; Nucl. Phys. B **194** (1982) 445.

[2] J. C. Collins, D. E. Soper and G. F. Sterman, Adv. Ser. Direct. High Energy Phys. **5**, 1 (1989).

[3] S. Albino, Rev. Mod. Phys. **82**, 2489 (2010); A. Metz and A. Vossen, Prog. Part. Nucl. Phys. **91**, 136 (2016).

[4] R. D. Ball *et al.* [NNPDF Collaboration], JHEP **1504**, 040 (2015).

[5] E. R. Nocera *et al.* [NNPDF Collaboration], Nucl. Phys. B **887**, 276 (2014).

[6] V. Bertone *et al.* [NNPDF Collaboration], in preparation.

[7] D. Buskulic *et al.* [ALEPH Collaboration], Z. Phys. C **66** (1995) 355.

[8] P. Abreu *et al.* [DELPHI Collaboration], Eur. Phys. J. C **5** (1998) 585.

[9] R. Akers *et al.* [OPAL Collaboration], Z. Phys. C **63** (1994) 181.

[10] R. Brandelik *et al.* [TASSO Collaboration], Phys. Lett. **94B** (1980) 444.

[11] M. Althoff *et al.* [TASSO Collaboration], Z. Phys. C **17** (1983) 5.

[12] W. Braunschweig *et al.* [TASSO Collaboration], Z. Phys. C **42** (1989) 189.

[13] M. Leitgab *et al.* [Belle Collaboration], Phys. Rev. Lett. **111** (2013) 062002.

[14] R. Itoh *et al.* [TOPAZ Collaboration], Phys. Lett. B **345** (1995) 335.

[15] J. P. Lees *et al.* [BaBar Collaboration], Phys. Rev. D **88** (2013) 032011.

[16] M. Derrick *et al.*, Phys. Rev. D **35** (1987) 2639.

[17] H. Aihara *et al.* [TPC/Two Gamma Collaboration], Phys. Rev. Lett. **61** (1988) 1263.

[18] K. Abe *et al.* [SLD Collaboration], Phys. Rev. D **69** (2004) 072003.

[19] X. Q. Lu, PhD Thesis, Johns Hopkins University, Baltimore, 1986.

[20] G. D'Agostini, Nucl. Instrum. Meth. A **346** (1994) 306.

[21] R. D. Ball *et al.* [NNPDF Collaboration], JHEP **1005** (2010) 075.

[22] P. J. Rijken and W. L. van Neerven, Nucl. Phys. B **487**, 233 (1997).

[23] N. Hansen, "The CMA evolution strategy: A tutorial", [arXiv:1604.00772 [cs.LG]].

[24] M. Epele, C. A. Garcia Canal and R. Sassot, Phys. Rev. D **94**, no. 3, 034037 (2016). [arXiv:1604.08427 [hep-ph]].

[25] V. Bertone, S. Carrazza and J. Rojo, Comput. Phys. Commun. **185**, 1647 (2014). [arXiv:1310.1394 [hep-ph]].

[26] V. Bertone, S. Carrazza and E. R. Nocera, JHEP **1503**, 046 (2015). [arXiv:1501.00494 [hep-ph]].

[27] M. Hirai, H. Kawamura, S. Kumano and K. Saito, PTEP **2016**, no. 11, 113B04 (2016) [arXiv:1608.04067 [hep-ph]].

[28] D. P. Anderle, T. Kaufmann, F. Ringer and M. Stratmann, arXiv:1611.03371 [hep-ph].